

Microstructure Evolution of Polycrystalline Pure Nickel during Static Recrystallization

Makoto Hasegawa and Hiroshi Fukutomi

Reprinted from

MATERIALS TRANSACTIONS, VOL. 43 NO. 9, SEPTEMBER, 2002

THE JAPAN INSTITUTE OF METALS

Aoba Aramaki, Aoba-ku, Sendai 980-0845, Japan

Microstructure Evolution of Polycrystalline Pure Nickel during Static Recrystallization *1

Makoto Hasegawa *2 and Hiroshi Fukutomi

Division of Materials Science and Engineering, Graduate School of Yokohama National University, Yokohama 240-8501, Japan

The difference in mechanisms of microstructure formation between static and dynamic recrystallization in pure nickel was studied on the basis of texture and EBSD analyses. Uniaxial compression was conducted at room temperature, followed by annealing at 905 K from 10 s to 28.8 ks. The process of static, primary recrystallization was traced by optical microscopy and the measurement of micro-Vickers hardness. Fraction of statically recrystallized region was 30% and 80% at annealing for 10 s and 60 s, respectively. Annealing longer than 60 s results in a 100% recrystallized state. The value of maximum pole density of texture was 4.6 after the uniaxial compression up to the true strain of -0.66 . During static recrystallization, the texture became weak and finally the maximum pole density fell off in 2.0. The position of maximum pole density, however, did not change from (011) (compression plane). At the early stage of static recrystallization, new grains nucleated with random orientation in the vicinity of grain boundaries, inhomogeneously deformed regions. On the other hand, at the later stage of static recrystallization, new grains formed from the regions suffered from relatively homogeneous deformation. At this stage, the main component of the texture was (011) though the texture itself was weak. In dynamic recrystallization, new grains nucleated with random orientation during the deformation giving high values of Zener-Hollomon parameter. It was concluded that, during dynamic recrystallization, the deformation proceeded and hence inhomogeneously deformed regions continuously formed in the vicinity of grain boundaries, resulting the preferential formation of new grains.

(Received May 9, 2002; Accepted July 8, 2002)

Keywords: polycrystalline pure nickel, static recrystallization, dynamic recrystallization, texture, electron backscattering pattern, random nucleation, uniaxial compression, inhomogeneous deformation

1. Introduction

Static recrystallization (hereafter abbreviated as SRX) and dynamic recrystallization (DRX) in metals are defined as the recrystallization occurring during annealing after plastic deformation and during high temperature deformation, respectively. Although SRX and DRX are similar phenomena in a viewpoint that the new grains are formed in the deformed matrix, only a few works have been done to know the difference in the microstructure formation process in SRX and DRX, that is the effect of simultaneous deformation on the microstructure formation.¹⁾

The mechanism of new grain formation under DRX that occurs during high temperature, uniaxial compression of polycrystalline pure nickel has been examined by the present authors.^{2,3)} It was found that new grains form in the vicinity of grain boundaries, where the deformation is inhomogeneous, with random orientation throughout the whole process of DRX in a deformation condition of low temperature and high strain rate. For SRX, on the other hand, it has been reported that the nucleation site of new grains⁴⁾ and also the recrystallization texture⁵⁾ change with the degree of cold working before recrystallization annealing. However, most of works on SRX were done for a rather large prestrain. For understanding the difference in the microstructure formation process between DRX and SRX, an experiment on SRX after deformation to a smaller strain that nearly equals the initiation strain of DRX, *i.e.* about 1.0 in true strain or less, is desired, though such works are few.

In previous experimental works on SRX, rolling was usually used as cold working prior to the annealing. However, cold rolling develops the so-called rolling texture having one of the main component $\{123\}$ $\{634\}$ ⁵⁾ characterized by both preferentially oriented rolling plane and rolling direction, so there arises a possibility that the orientation distribution of new grains varies from that of initially nucleated grains because of the preferential grain growth in the rolling-textured matrix. In this study, therefore, uniaxial compression was used as cold working; it develops the so-called fiber texture but any oriented new grains would not be in a special relationship of preferential growth to the fiber-textured matrix.

The present authors have considered that the characterization of both the microstructure and crystal orientation is necessary for understanding the process of microstructure formation during recrystallization.^{2,3)} The purpose of this work is to understand the process of SRX in a range of primary recrystallization and make clear the difference between SRX and DRX from a microstructural viewpoint.

2. Experimental Procedure

Pure nickel of 99.9 mass% purity was used for the test. Cylindrical specimens with a diameter of 8 mm and a height of 12 mm were machined from a cold drawn rod and annealed at 1073 K for 3.6 ks. The average grain size after the annealing was 80 μm . Uniaxial compression tests were conducted at room temperature (293 K) under a true strain rate of $1.0 \times 10^{-3} \text{ s}^{-1}$ up to desired strains. Annealing of compressed specimens were carried out in a salt bath (CaCl₂ 46, NaCl 54 in mass%) at a temperature of 905 K for various periods (10 s, 15 s, 20 s, 30 s, 60 s, 0.3 ks, 0.6 ks, 1.8 ks, 3.6 ks, 7.2 ks and 28.8 ks). After annealing, the specimens were dropped

*1 This Paper was Originally Published in J. Japan Inst. Metals 66 (2002) 40-45.

*2 Graduate Student, Yokohama National University. Present address: Institute of Industrial Science, The University of Tokyo. Tokyo 153-8505, Japan.

into water for quenching the microstructure. After the tests, mid-plane sections of the specimens were prepared by mechanical polishing. Microstructure was observed by optical microscopy and SEM after chemical etching. Measurement of Vickers hardness was also conducted on the mid-plane sections.

Texture measurement was performed on the mid-plane sections by the Schulz-reflection method using nickel filtered Cu-K α radiation. The diffracted X-ray intensities were measured on 111, 200 and 220 reflections and {111}, {200} and {220} pole figures were constructed. Based on these three pole figures, an ODF (orientation distribution function) was calculated by the Dahms-Bunge method.⁶⁾ The main component and the sharpness of the texture were determined from inverse pole figures derived from the ODF.

Orientation measurements by EBSP technique were done at intervals of 2 μm , and minimum rotation angles θ between neighboring points of measurement were calculated. When θ is between 5° and 12°, it was judged that a low angle boundary exists between the two points. When θ is larger than 12°, the boundary was defined as a high angle grain boundary. Figures of high angle grain boundaries were drawn from results of the above mentioned orientation measurements. The figures are called "grain structure micrographs" in the present paper. The lower limit of θ for a high angle boundaries (12°) was chosen since the grain structure micrograph well coincides with the micrograph obtained by optical microscopy and SEM.

Recrystallized grains and unrecrystallized grains can be distinguished from their size at the early stage of SRX; the former is smaller than the latter. At the later stage of SRX, however, the recrystallized grains may possibly be larger than the unrecrystallized grains because of the migration of grain boundaries of recrystallized grains into the surrounding, unrecrystallized region. In this case, both kinds of grains cannot be distinguished only from their size. Concerning the misorientation distribution within the grains, however, it should be always larger in the unrecrystallized grains because of a higher density of dislocations introduced during cold working, even though the dislocation structure has been thermally recovered. In this study, therefore, recrystallized grains and unrecrystallized grains were distinguished not only from the microstructure but also from the average misorientation.

The average misorientation was defined as an average angle of misorientation between the neighboring two points of orientation measurement in one grain. Figure 1 is a histogram showing a relationship between the average misorientation (abscissa) and its frequency represented by the area fraction of grains (ordinate). Specimens were deformed at room temperature up to a true strain of -0.66 (Fig. 1(a)) and then fully annealed at 905 K for 7.2 ks for the completion of primary recrystallization (Fig. 1(b)). In Fig. 1(a), the area fraction of grains takes a maximum in the misorientation between 2.4° and 2.8° and the misorientation minimum is in between 1.6° and 2.0°. In Fig. 1(b), on the other hand, the area fraction of grains takes a maximum in the misorientation between 0.4° and 0.8° and the misorientation maximum is in between 1.2° and 1.6°. Further, it can be seen in Fig. 1(b) that more than 99% of the recrystallized grains takes the misorientation less than 1.2°. Therefore, the value of misorientation of 1.2° was

taken as a critical value for distinguishing recrystallized and unrecrystallized grains.

3. Experimental Results

3.1 Changes in micro-Vickers hardness and microstructure during static recrystallization

Figure 2 shows a change in the micro-Vickers hardness with annealing at 905 K after compression at room tempera-

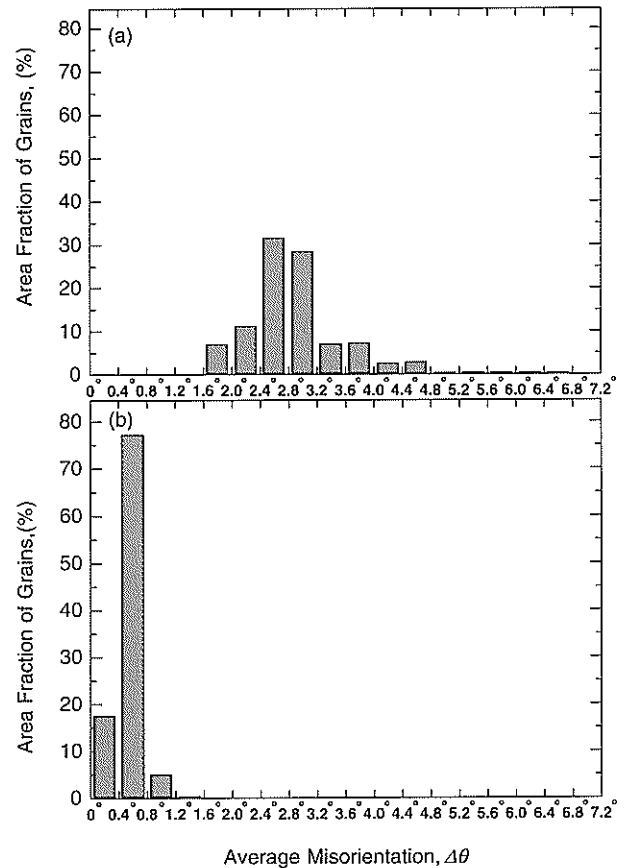


Fig. 1 Histogram showing the distribution of average misorientation in each grain by area fraction of grains. Compressed at room temperature up to a true strain of $\varepsilon = -0.66$ (a), followed by the annealing at $T = 905$ K for $t = 7.2$ ks (b).

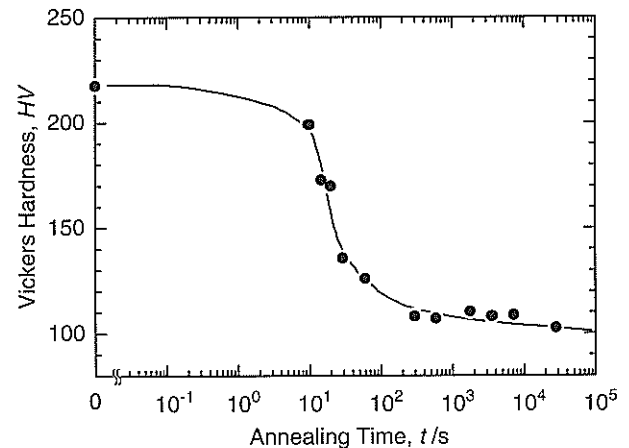


Fig. 2 Relationship between annealing time at $T = 905$ K and micro-Vickers hardness after compression at room temperature up to a true strain of $\varepsilon = -0.66$.

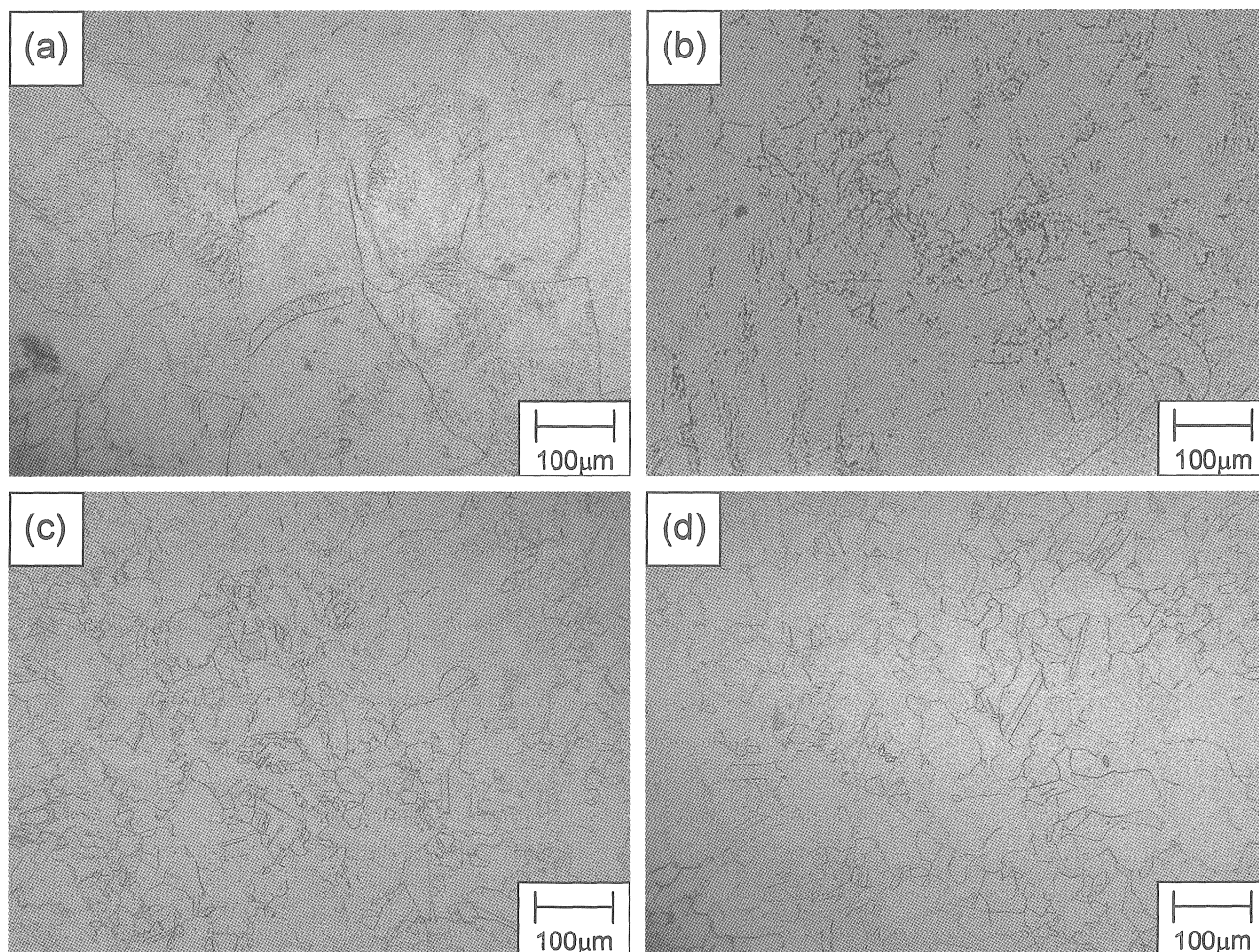


Fig. 3 Optical micrographs of pure nickel annealed at $T = 905$ K for various annealing times t after compression at room temperature up to a true strain of $\varepsilon = -0.66$. (a) As compressed, (b) annealed for $t = 15$ s, (c) annealed for $t = 60$ s and (d) annealed for $t = 7.2$ ks.

ture up to a true strain of -0.66 . The hardness after compression was $HV = 218$. It reduced slightly to 199 after annealing for 10 s, decreased rapidly during further annealing up to 0.3 ks and finally reached 107. The annealing times for taking micrographs to understand the change in microstructure during annealing were determined from the hardness-annealing time curve.

Optical micrographs taken before and after annealing for various times (15 s, 60 s and 7.2 ks) are given in Fig. 3(a) and Figs. 3(b) to (d), respectively. Microstructure developed by cold working is inhomogeneous as shown by the etched pattern in Fig. 3(a); severer deformation is seen in the vicinity of grain boundaries. After annealing for 15 s, the nucleation of new grains can be seen in the vicinity of initial grain boundaries; the fraction of recrystallized area is about 30% at this stage of SRX (Fig. 3(b)). After annealing for 60 s, about 80% of the area has been occupied by the SRXed grains, though some unrecrystallized large grains still remain (Fig. 3(c)). After annealing for 7.2 ks, all the area has been fully replaced by the SRXed structure (Fig. 3(d)). The average size of SRXed grains is $31 \mu\text{m}$ at this stage and the annealing twins can be seen in the microstructure.

The change in microstructure during SRX can be concluded from Figs. 2 and 3 as follows. The thermal recovery mainly occurs in the beginning of annealing (till 10 s),

and then new grains nucleate first in the vicinity of initial grain boundaries and later in the interior of initial grains. The primary recrystallization is completed during annealing for about 0.3 ks and the normal grain growth follows in the further annealing.

3.2 Texture

Inverse pole figures showing the distribution of pole densities of the compression plane are given in Fig. 4. The average densities are used as units. Figures 4(a) to (d) correspond to the microstructures shown in Figs. 3(a) to (d), respectively. The maximum pole density (P_{MAX}) and its position (α , β) are given below each figure. The definition of angles α and β is given in Fig. 4(e). In the microstructure developed in compression at room temperature up to a true strain of -0.66 (Fig. 4(a)), the value of P_{MAX} is 4.6 and the position of P_{MAX} is in (011) that is the stable orientation for compressive deformation. The value of P_{MAX} decreases to 3.9 after annealing at 905 K for 15 s (Fig. 4(b)). After annealing for 60 s and 7.2 ks, the values of P_{MAX} decrease to 2.3 (Fig. 4(c)) and 2.0 (Fig. 4(d)), respectively. The position of P_{MAX}, however, does not change from (011) during annealing. This means that, in the progress of SRX after uniaxial compression, the texture becomes weak but the main component remains in (011), that is the stable orientation for compression.

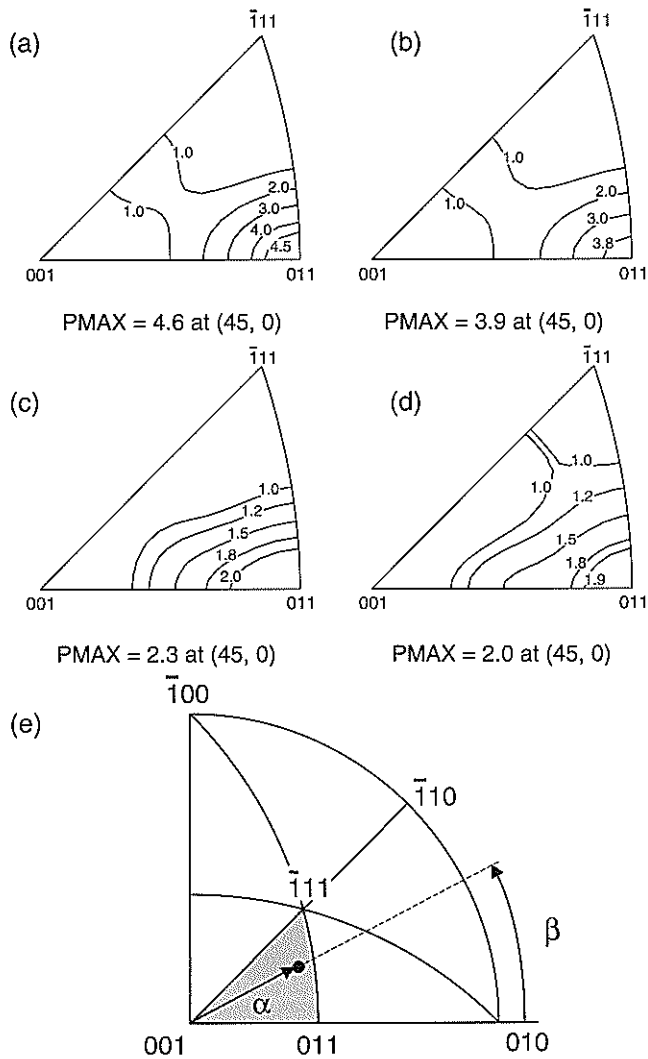


Fig. 4. Inverse pole figures showing the distribution of pole densities of the compression plane. The average densities are used as units. The compression was carried out at room temperature up to a true strain of $\epsilon = -0.66$ (a). After the compression, the annealing was conducted at $T = 905$ K for (b) $t = 15$ s, (c) $t = 60$ s and (d) $t = 7.2$ ks. The position of maximum pole density (α , β) is given below each figure. The definition of angles α and β is given in (e).

3.3 Change in the orientation distribution of recrystallized grains with the progress of SRX

Figure 5(a) shows the grain structure micrograph for the microstructure developed during annealing for 15 s (Fig. 3(b)), that is at the early stage of SRX. In the figure, thin lines are high angle grain boundaries ($\theta \geq 12^\circ$) and thick lines are $\Sigma 3$ coincidence grain boundaries (twin boundaries). Recrystallized grains and unrecrystallized grains are represented by white and dark areas, respectively. Almost all of the grain boundaries between recrystallized grains and unrecrystallized ones are high angle boundaries. In the case that recrystallized grains mutually adjoin, about a half of the grain boundaries between them are $\Sigma 3$ coincidence grain boundaries. Figure 5(b) shows the crystal orientation of recrystallized grains in the form of inverse pole figure in which the average densities are used as units. The position of PMAX disperses around the orientation of 17° away from (001) to (011), and the value of PMAX is only 1.5 times of the level for the random orientation distribution. These may indicate that the orientation

of recrystallized grains at the early stage of SRX is almost at random.

Figure 6(a) is the grain structure micrograph for the microstructure after 60 s annealing (Fig. 3(c)) at the later stage of SRX. Although the unrecrystallized grains (dark area) still remain, most of the area has been occupied by the recrystallized grains (white area). As at the early stage of SRX, almost all of the grain boundaries between recrystallized and unrecrystallized grains are high angle boundaries, and there are many $\Sigma 3$ coincidence boundaries between recrystallized grains. The crystal orientation of recrystallized grains is shown in Fig. 6(b) in the form of inverse pole figure. The value of PMAX is again not so high, only 1.7 times of the level for random orientation. In contrast to Fig. 5(b), however, the position of PMAX is in (011). In other words, newly formed grains have (011) orientation but construct high angle boundaries with unrecrystallized grains. Therefore, it may be reasonably considered that, at the later stage of SRX (primary recrystallization), new grains develop by the growth of small region within the unrecrystallized grains, accompanying the rotation around [011] axis.

4. Discussion

4.1 Difference in the recrystallization processes after rolling and compression

Texture formation during SRX has mainly been studied after rolling, not after compressive deformation, probably for the practical interest in the mechanism of cube texture formation. It is known at present for nickel that the sharp cube texture {001} {100} develops during annealing after heavy rolling (rolling rate: 88.9%), but the deformation texture remains in the recrystallized structure after light rolling (30.6 and 64.7%).⁵⁾

Although the mechanism of cube texture formation is still under discussion, it is usually considered that the area of cube orientation grows encroaching upon the deformed matrix of the S orientation {123} {634} that is one of the main components of the rolling texture. In this case, the orientation of recrystallized area and that of deformed matrix are in a relationship of favoring growth accompanying 40° rotation around the common $\langle 111 \rangle$ axis (hereafter written as “ 40° $\langle 111 \rangle$ favoring growth”). This relationship has been reported to hold not only for the unidirectional rolling but also for the compression rolling.⁷⁾

On the other hand, in contrast to the SRX texture after rolling (cube texture), the main component of the SRX texture after uniaxial compression is the same as that of deformation texture (011). In addition, it has been reported⁵⁾ that, even after rolling, the deformation texture still remains in the fully SRXed structure if the rolling rate is low. Therefore, one might argue that no change in the main component of texture (011) during SRX after uniaxial compression (Figs. 4(d) and 6(b)) is ascribed to a rather small compressive strain of -0.66 which corresponds to 48% in the rolling rate.

To answer this question, the SRX texture was examined after compression up to a larger strain of -1.7 that corresponds to the rolling rate of 82%. Inverse pole figures taken before and after the annealing at 905 K for 3.6 ks are given in Figs. 7(a) and (b), respectively. The value of PMAX is 5.6

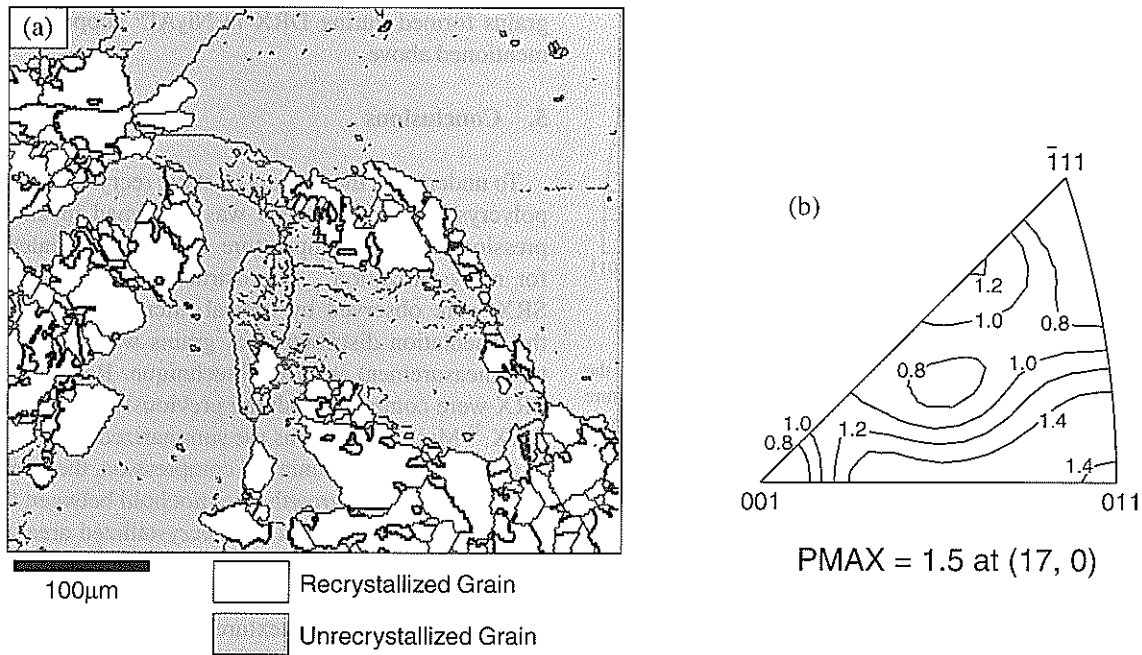


Fig. 5 Grain structure micrograph, constructed by EBSD, annealed at $T = 905$ K for $t = 15$ s after compression at room temperature up to a true strain of $\epsilon = -0.66$ (a) and the inverse pole figure of recrystallized grains nucleated by the time (b). —: high angle boundary, ———: twin boundary.

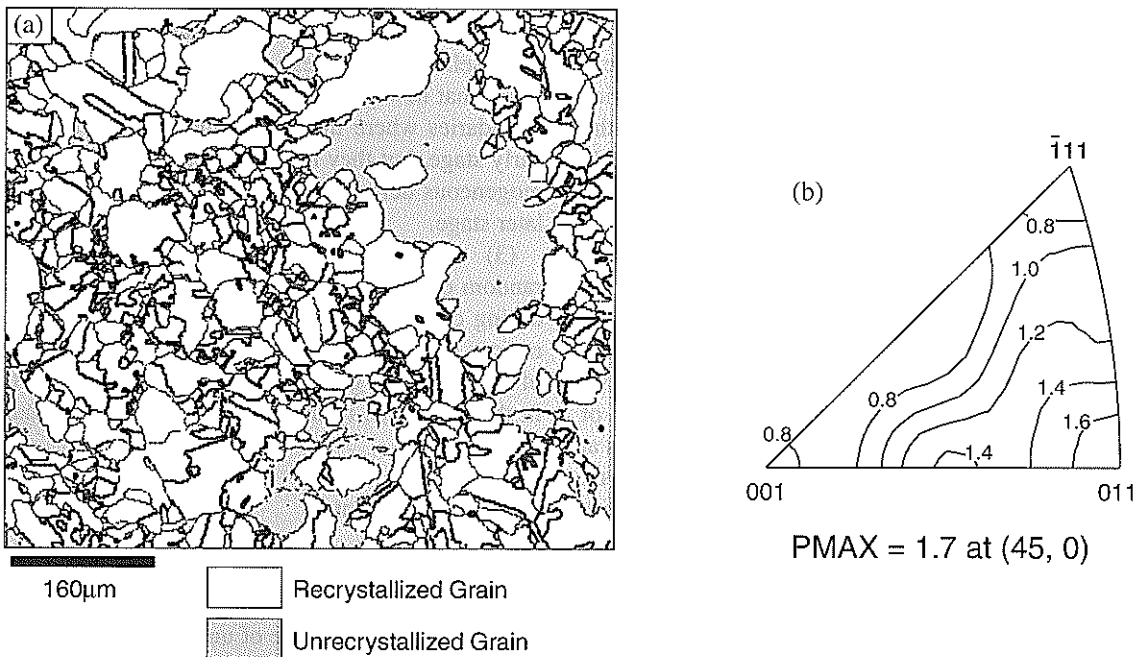


Fig. 6 Grain structure micrograph, constructed by EBSD, annealed at $T = 905$ K for $t = 60$ s after compression at room temperature up to a true strain of $\epsilon = -0.66$ (a) and the inverse pole figure of recrystallized grains nucleated by the time (b). —: high angle boundary, ———: twin boundary.

in the as-deformed state and decreases to 2.9 by the annealing. However, the position of P_{MAX} remains in (011) during SRX. This indicates that, in contrast to the case of rolling, the relationship of 40° (111) favoring growth does not hold in the SRX after uniaxial compression. In other words, no preferentially oriented grain growth occurs because the fiber texture formed by uniaxial compression has various orientations in the directions making a right angle to the compressive axis [011]. Hence, the examination of SRX after uniaxial compression may be useful for understanding the nature of new

grain formation in the deformed matrix.

4.2 Process of static recrystallization

The formation of new grains in SRX is known to occur preferentially in the regions of inhomogeneous deformation such as the vicinity of grain boundaries, deformation bands and/or shear bands.⁴⁾ In fact, after compression up to -0.66 in true strain, new grains were found in the vicinity of initial grain boundaries as seen in Figs. 3(b) and 5(a). At the present stage, the microstructure evolution and texture devel-

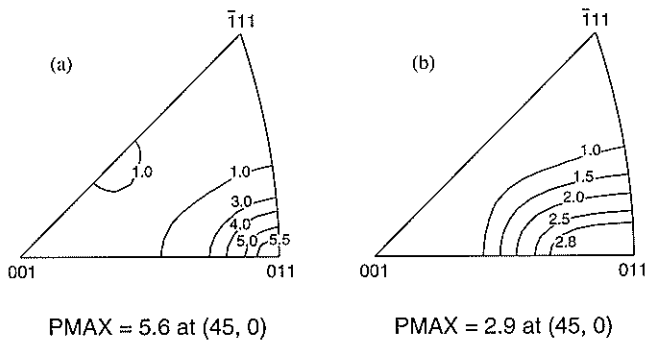


Fig. 7 Inverse pole figures showing the distribution of pole densities of the compression plane. The compression was carried out at room temperature up to a true strain of $\epsilon = -1.7$ (a). After compression, the annealing was conducted at $T = 905$ K for $t = 3.6$ ks (b).

opment during SRX in nickel can be understood summarily as follows.

The deformation in the vicinity of grain boundaries is essentially inhomogeneous because of the plastic constraint due to grain boundaries; more slip systems are activated and local dislocation density becomes higher compared to the interior of grains. Therefore, at the early stage of SRX, new grains nucleate with random orientation in the vicinity of initial grain boundaries. In the subsequent growth of new grains, twinning occurs in succession during grain boundary migration, as expected from Fig. 5(a) where about a half of mutual boundaries between recrystallized grains were twin boundaries. At the later stage of SRX, the formation of new grains with (011) orientation occurs in the regions of relatively homogeneous deformation, that is in the grain interior. Of course, even in the grain interior, very small, inhomogeneously deformed regions may exist, and the nucleation of new grains with random orientation may occur in these regions. However, the preferential growth of such grains may not occur because the relationship of $40^\circ \langle 111 \rangle$ favoring growth does not hold. As a result, most of new grains have the orientation distribution of (011) that is the stable orientation for the compression. As at the early stage of SRX, twinning occurs during grain growth. This may be the reason why the value of PMAX reduces with the progress of SRX, though the position of PMAX remains at (45, 0) (Figs. 4 and 7).

4.3 Effect of concurrent deformation on the recrystallization behavior

Let us compare here the process of SRX with that of dynamic recrystallization (DRX) that occurs during plastic deformation.³⁾ The formation process of new grains is similar both in SRX and DRX; new grains form in the vicinity of initial grain boundaries. In the case of SRX, inhomogeneously deformed regions near grain boundaries are first consumed by the new grain formation and further formation of new grains at the later stage occurs in the uniformly deformed regions, that is in the grain interior. In the case of DRX, however, the concurrent deformation continues to develop the inhomogeneous microstructure in the vicinity of newly formed grains. Therefore, the orientation distribution of the newly nucleated grains is always at random even at the later stage of DRX. The result on the orientation distribution of new

grains formed during DRX in Ni_3Al ⁸⁾ supports the concept mentioned above.

5. Conclusions

To understand the process of static recrystallization (SRX), polycrystalline pure nickel was deformed in uniaxial compression at room temperature and then annealed at 905 K for recrystallization. Microstructures at various stages of SRX were observed by optical microscopy and SEM, and the orientation distribution of grains was examined by texture measurement and EBSD technique. Results obtained for SRX were compared with the previously obtained results for DRX.³⁾ Main conclusions are summarized as follows.

(1) In SRX after uniaxial compression, the relationship of $40^\circ \langle 111 \rangle$ favoring growth does not hold between the orientations of deformed matrix and recrystallized area, in contrast to the case of pre-deformation by rolling. This may be due to a fact that the preferentially oriented grain growth does not occur because the fiber texture formed by the uniaxial compression has various orientations in the directions that make a right angle to the compressive axis [011].

(2) At the early stage of SRX, the orientation distribution of new grains is at random. At the later stage, however, the main component of new grains takes (011), though the texture itself is weak. These phenomena can be understood from a fact that new grains nucleate in the vicinity of initial grain boundaries where the deformation is inhomogeneous at the early stage, but they nucleate in the regions of relatively homogeneous deformation, namely in the grain interior, at the later stage.

(3) In contrast to SRX, new grains always nucleate with random orientation in DRX. This may be due to a fact that, during concurrent deformation, inhomogeneously deformed regions continue to develop in the vicinity of grain boundaries of newly formed grains and new grains nucleate in succession in these regions, resulting in the random orientation of new grains.

Acknowledgements

The authors would like to express their thanks to Dr. S. Takagi of Industrial Research Institute of Kanagawa for his help in using the machine of uniaxial compression tests. This work was financially supported by JSPS research for the future program. The authors greatly appreciate to the program.

REFERENCES

- 1) T. Maki and I. Tamura: *J. Iron Steel Inst. Japan* **70** (1984) 2073–2080.
- 2) H. Fukutomi, M. Hasegawa and M. Yamamoto: *J. Japan Inst. Metals* **65** (2001) 71–77.
- 3) M. Hasegawa and H. Fukutomi: *Mater. Trans.* **43** (2002) 1183–1190.
- 4) K. Ito: *J. JILM* **31** (1981) 497–507.
- 5) J. Pospiech, J. Jura, A. Mücklich, K. Pawlk and M. Betzl: *Textures and Microstructures* **6** (1983) 63–80.
- 6) M. Dahms and H. J. Bunge: *J. Appl. Cryst.* **22** (1989) 439–447.
- 7) H. Inoue, Y. Yoshida and N. Inakazu: *J. JILM* **44** (1994) 646–651.
- 8) D. Ponge and G. Gottstein: *Acta Mater.* **46** (1998) 69–80.